Available online at www.sciencedirect.com
ScienceDirect
Journal of Molecular Catalysis A: Chemical 275 (2007) 63–71
JOURNAL OF MOLECULAR CATALYSIS A: CHEMICAL
www.elsevier.com/locate/molcata

Interactions of methane, ethane and pentane with the (110C) surface of γ-alumina

Shuhui Cai [a,b], Viorel Chihaia [c], Karl Sohlberg [b,*]

[a] *Department of Physics, State Key Laboratory of Physical Chemistry of Solid Surface, Xiamen University, Xiamen 361005, PR China*
[b] *Department of Chemistry, Drexel University, Philadelphia, PA 19104, USA*
[c] *I.G. Murgulescu Institute of Physical Chemistry of the Romanian Academy, Spl. Independentei 202, 060041 Bucharest, Romania*

Received 25 November 2006; received in revised form 18 April 2007; accepted 15 May 2007
Available online 21 May 2007

Abstract

Adsorptions of methane, ethane and pentane on the γ-alumina (110C) surface are investigated with semi-empirical (PM3) cluster calculations. It is found that the abstraction of an H atom accompanied by the formation of a C–O bond is the most favorable reaction for methane on the alumina surface. For ethane– and pentane–alumina interactions, the abstraction of two H atoms accompanied by the formation of an alkene is the most favorable reaction. The surface Al atoms help to promote the reactions, but are not directly involved in the bond formation.

Keywords: Chemisorption; Methane; Ethane; Pentane; Semi-empirical calculations; γ-Alumina

1. Introduction

The interpretation of H/D exchange between surface OH-groups of a metal oxide and CD_4 as an indication of strong Brönsted acidity [1–4] was questioned by Engelhardt et al. [5,6], who proposed an alternative explanation that H/D exchange could be initiated by dissociative methane chemisorption over Lewis acid–Lewis base pair sites. Such chemisorption would produce the surface species $CD_3^{\delta-}$ and $D^{\delta+}$, with the $CD_3^{\delta-}$ moiety bound to a valence unsaturated Al atom of Lewis acid character.

The Lewis acidity of surface Al sites on γ-alumina has been the subject of several previous investigations [7–9], as has the reactivity of these sites with water [10–12], hydrogen sulfide [10], carbon monoxide [10], ammonia [11], pyridine [11], and methanol [13]. Previously we applied theoretical calculations to gain insight into the interaction of 1-hexene with γ-alumina, and found the interaction to be purely repulsive at valence unsaturated surface Al sites [14]. By contrast, investigations of the interactions of simple alcohols with γ-alumina showed participation of the surface Lewis acid sites [15].

Herein we report the results of calculations designed to investigate the adsorption of methane, ethane and pentane on the γ-alumina (110C) surface. Two cluster models, $H_8Al_{40}O_{64}$ (which exposes an Al–O terminated face on the hydrogen-spinel form of γ-alumina) and $Al_{48}O_{72}$ (which exposes an oxygen terminated face on the hydrogen-free defect-spinel form of γ-alumina), were used to model the γ-alumina surface. By employing models with different degrees of hydrogenation we can explore the temperature dependence of the reactivity of γ-alumina as a heterogeneous catalyst. We found that on both models, the most energetically favorable first reaction step for methane is H abstraction from the carbon (C1) position, with C1 bonding to a surface oxygen. (*Note*: atomic labels are C1–C2–C3–C4–C5 for pentane, C1–C2 for ethane and C1 for methane. H*n* refers to the H atoms bonding to C*n*.) For ethane and pentane, the most energetically favorable first reaction step is the dehydrogenation of two H atoms from different carbon atoms. In pentane–alumina interactions, the two H atoms are abstracted from C2 and C3, respectively, producing 2-pentene. Under certain conditions these reactions can be exothermic. The lowest energy barriers to these reactions are around 60–70 kcal/mol on $H_8Al_{40}O_{64}$ model and around 26–37 kcal/mol on $Al_{48}O_{72}$ model.

* Corresponding author. Tel.: +1 215 895 2653; fax: +1 215 895 1265.
E-mail address: sohlbergk@drexel.edu (K. Sohlberg).

1381-1169/$ – see front matter © 2007 Elsevier B.V. All rights reserved.
doi:10.1016/j.molcata.2007.05.025

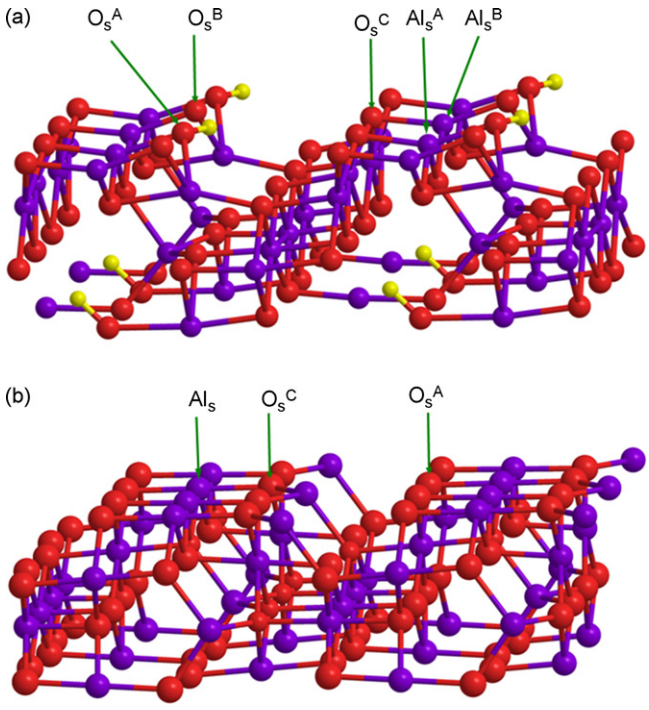

Fig. 1. Cluster models used in this study. (a) Model I: an Al–O terminated surface; (b) Model II: an oxygen terminated surface. The purple, red and yellow spheres represent Al, O, and H atoms, respectively. (For interpretation of the references to color in this figure legend, the reader is referred to the web version of the article.)

2. Computational method and models

The adsorptions of methane, ethane and pentane on the γ-alumina (110C) surface were investigated with electronic structure calculations based on the semi-empirical PM3 Hamiltonian [16,17] and $H_8Al_{40}O_{64}$ and $Al_{48}O_{72}$ cluster models of γ-alumina (see Fig. 1). We chose the PM3 model Hamiltonian because it is parameterized for Al and because the much lower computational cost of semi-empirical calculations allows for modeling a cluster that includes all atoms up to and including second-nearest-neighbors of the adsorption site, much larger than is currently practical with first-principles methods. The large cluster size is important because second-nearest-neighbor effects have been shown to heavily influence surface chemistry in cubic aluminas [18]. Semi-empirical models have been used effectively in theoretical investigations of similar systems [8,15,19,20] and have been shown to lead to qualitative conclusions and energetic behavior consistent with first-principles calculations.

γ-Alumina has been described as a defect-spinel structure closely related to that of Mg-spinel (space group $Fd\bar{3}m$) [21] but with the Al cations distributed over both the octahedral (O_h, Al sites) and tetrahedral (T_d, Mg sites) interstitial sites within the oxygen anion sublattice. γ-Alumina has a range of valid stoichiometries $H_{3m}Al_{2-m}O_3$ ($0 \leq m \leq (1/3)$), but the lowest energy form has the stoichiometry of a hydrogen–aluminum spinel [22]. The primitive unit cell of the lowest energy form is HAl_5O_8, where the H atom and one Al atom occupy (nominally) the Mg sites in the spinel structure, and the remaining four Al atoms occupy the Al sites in the spinel structure. Surface studies show that the (110C) layer of γ-alumina is preferentially exposed [23–26]. The $H_8Al_{40}O_{64}$ cluster model [14] (Model I, Fig. 1(a)) was constructed based on structural relaxation studies of a 56-atom slab of γ-alumina (HAl_5O_8 stoichiometry) four atomic layers thick [18]. This is representative of γ-alumina at low to moderate temperatures. The $Al_{48}O_{72}$ cluster model (Model II, Fig. 1(b)) is constructed based on the $Al_{48}O_{64}$ supercell of hydrogen-free γ-alumina. The cation vacancies required for valence balance were assigned to tetrahedral sites parallel to the (110C) surface [15]. This model is representative of the γ-alumina surface at high temperatures. These two models ensure that the coordination environment of the surface atoms interacting with the adsorbate, and their nearest-neighbors, are representative of those on the surface of the periodic crystal.

For Model I, two different surface aluminum sites for alkane adsorption were studied as indicated in Fig. 1(a). Only surface Al atoms at O_h sites were considered since three-coordinated Al practically does not exit on the surface [26–28]. At site A, the surface Al atom interacting with the alkane has a neighboring OH. (Denoted as Al_s^A. The subscript "s" indicates an atom on the alumina surface.) At site B, there is no neighboring OH around the Al atom that interacts with alkane (denoted as Al_s^B). Interactions of an alkane with three different surface O sites were considered as indicated in Fig. 1(a). At site A, the surface O atom is coordinated by one H atom and two Al atoms (denoted as O_s^A). At site B, the surface O atom is coordinated by two Al atoms (denoted as O_s^B). At site C, the surface O atom is coordinated by three Al atoms (denoted as O_s^C). As previous density-functional calculations have shown no appreciable relaxation effects or consequence for surface atoms, with the exception of the three-coordinated Al atoms that are not considered here [26], the alumina substrate was frozen in all calculations with the exception of the H atom bound to the O_s^A atom.

For Model II, the slab is free of H atoms so Al_s^A and Al_s^B atoms are equivalent, as are O_s^A and O_s^B (see Fig. 1(b)). Therefore, we only consider Al_s, O_s^A and O_s^C sites. The alumina substrate was frozen in all calculations.

In structural optimizations, the adsorbed molecules were fully relaxed, including their positions relative to the surface, except in the case of energy barrier calculations where one of the H1–O_s distances was fixed at different values from about 0.1 to 0.5 nm in steps of approximately 0.02 nm. For all chemisorbed states, vibrational frequencies were calculated to ensure that each state is a true local minimum.

To study molecule/surface interactions the free molecule was placed in close proximity to the surface in various orientations and for each orientation a geometry optimization was carried out. We specify the interaction as A–X_s. This notation denotes atom A of the free molecule in close proximity to atom X_s of the surface slab. In some cases the initial orientation of the free molecule involved two close contacts, denoted as A–X_s & B–Y_s, where atom A of the free molecule is in close proximity to atom X_s of the surface slab and atom B of the free molecule is simultaneously in close proximity to atom Y_s of the surface slab. The following possible interaction modes were investigated: (1)

an H1 atom interacts with a surface Lewis base site (H1–O_s); (2) the C1 atom interacts with an O_s site (C1–O_s); (3) the C1 atom and an H1 atom interact with a same O_s site (H1–O_s & C1–O_s); (4) the C1 atom and an H1 atom interact with two different O_s sites (C1–O_s^i & H1–O_s^j); (5) the C1 atom interacts with an Al_s site and an H1 atom interacts with an O_s site (C1–Al_s & H1–O_s); (6) an H1 and an H2 atom interact with two O_s sites (H1–O_s^i & H2–O_s^j); (7) an H2 atom interacts with an O_s site (H2–O_s); (8) an H3 atom interacts with an O_s site (H3–O_s); (9) an H2 and an H3 atom interact with two different O_s sites (H2–O_s^i & H3–O_s^j). (Interaction mode 6 is only available for ethane and pentane. Interaction modes 7, 8 and 9 are available only for pentane.) The superscripts i and j indicate two different sites. The initial C1–O_s and H–O_s distances were set to less than 0.15 and 0.1 nm, respectively to allow for strong interaction.

3. Results

The calculated results are given in Table 1 .

3.1. Adsorption of methane, ethane and pentane on Model I

3.1.1. Interactions of H1 with a surface O atom

When the initial configuration is such that one of the H1 atoms of methane, ethane or pentane is in close proximity to a surface oxygen atom (with sufficiently short H–O_s distances for strong interactions), upon full relaxation the molecule simply leaves the surface without any reaction.

3.1.2. Interactions of C1 with a surface O atom

Instead of an H1 atom as in Section 3.1.1, we placed the C1 atom close to a surface oxygen atom. Similarly, no reactions happen upon full optimization.

3.1.3. Interactions of H1 and C1 with a surface O atom

Reactions were found to happen in the cases of H1–O_s^A & C1–O_s^A and H1–O_s^B & C1–O_s^B. In both cases, upon full optimization the H1–C1 bond is broken and both the H1 and C1 atoms bond to the same O_s atom. The length of the newly formed H1–O_s bond is about 0.1 nm, while the C1–O_s bond length is 0.146–0.163 nm (see Table 1), indicating a chemisorbed state. The energies of these final chemisorbed states, however, are higher than that of the corresponding free state [E(alkane) + E($H_8Al_{40}O_{64}$)], i.e. these reactions are endothermic. Note that for these reactions, the H_s that was originally bonded to O_s^A moves to a nearby O_s (if the O_s^A is involved in reaction) due to strong repulsive interaction between H_s and nearby C or H atoms in the initial state. As shown in Table 1, this typically has the effect of significantly decreasing ΔE for chemisorption.

To estimate the energy barriers for such reactions, we fixed the H1 atom at various positions relative to O_s and relaxed all other atoms of the molecule. The energy variation with the H1–O_s distance can then be mapped out. Fig. 2 shows the energy variation with H1–O_s distance for the H1–O_s^A & C1–O_s^A interaction, where $\Delta E = E$(alkane/$H_8Al_{40}O_{64}$) $- E$(alkane) $- E$($H_8Al_{40}O_{64}$). The energy increases with the decrease of H1–O_s distance before reaction. For the H1–O_s^A & C1–O_s^A interaction, the energy required for a free molecule to come to a surface position close enough for the reaction to happen is 94.2, 101.4 and 107.7 kcal/mol for methane, ethane and pentane, respectively. This implies that there is an energy barrier to overcome before the chemisorbed state, where dehydrogenation occurs, is accessed. The interactions at site O_s^B are similar to site O_s^A, but the dehydrogenated state is even higher in energy. The energy decrease in the final state for the H1–O_s^A & C1–O_s^A interaction is mainly due to the transfer of H_s on the O_s^A to another O_s atom.

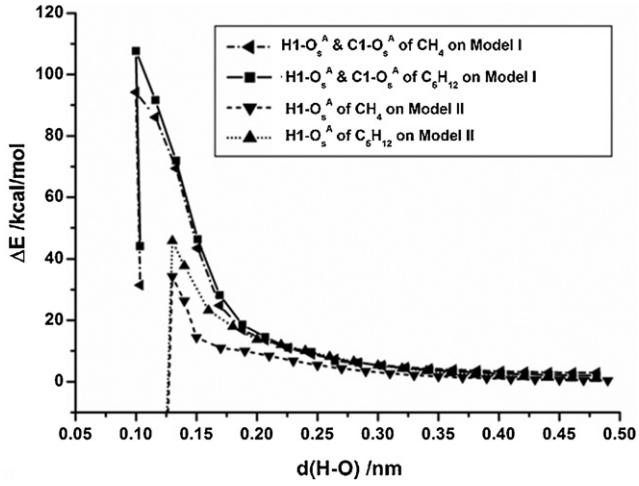

Fig. 2. Examples of energy variations with H–O_s distance for alkane–alumina interactions. Symbols indicate the computed points. The lowest energy points are corresponding to full relaxation structures.

3.1.4. Interactions of H1 and C1 with two different surface O atoms

Methane, ethane and pentane can all react with surface oxygen atoms by simultaneous interaction of H1 & C1 with two different O_s^C atoms, but their final states are different. For methane, in addition to H1 dehydrogenation, the C1 atom bonds to the nearby O_s atom; while for ethane and pentane, the remnant fragment leaves the surface after dehydrogenation. The newly formed H–O_s bond lengths are 0.097 nm, and the C1–O_s bond length is 0.14 nm. These reactions are endothermic. The reactions of methane, ethane and pentane with O_s^A & O_s^B are all similar to that of methane with O_s^{C1} & O_s^{C2} except that it is exothermic due to the transfer of the H_s atom on the O_s^A to another O_s atom. (The superscripts C1 and C2 indicate two different O^C sites. The initial and final state configurations of the C1–O_s^A & H1–O_s^B interaction for methane are shown in Fig. 3.)

Similar energy barrier calculations to those described in Section 3.1.3 show that the energy required for the reactions of methane and ethane on O_s^A & O_s^B to happen are lower than that on O_s^{C1} & O_s^{C2}, whereas that for pentane on O_s^A & O_s^B is higher than that on O_s^{C1} & O_s^{C2}.

Table 1
Results of various kinds of interactions (distances in nm and energies in kcal/mol)

No.	Alkane	Initial close contact		Bond formed				ΔE	ΔE_{act}
Model I									
1		H1–O_s		No reaction					
2		C1–O_s		No reaction					
3		H1–O_s & C1–O_s							
	CH_4	H1–O_s^A	C1–O_s^A	H1–O_s^A (0.104)	C1–O_s^A (0.146)	H_s transfer		31.5	94.2
	C_2H_6	H1–O_s^A	C1–O_s^A	H1–O_s^A (0.103)	C1–O_s^A (0.148)	H_s transfer		40.7	101.4
	C_5H_{12}	H1–O_s^A	C1–O_s^A	H1–O_s^A (0.103)	C1–O_s^A (0.149)	H_s transfer		44.1	107.7
	CH_4	H1–O_s^B	C1–O_s^B	H1–O_s^B (0.105)	C1–O_s^B (0.155)			115.8	115.8
	C_2H_6	H1–O_s^B	C1–O_s^B	H1–O_s^B (0.104)	C1–O_s^B (0.163)			123.6	123.6
	C_5H_{12}	H1–O_s^B	C1–O_s^B	H1–O_s^B (0.104)	C1–O_s^B (0.162)			126.5	126.5
		H1–O_s^C	C1–O_s^C	No reaction					
4		C1–O_s^i & H1–O_s^j							
	CH_4	C1–O_s^A	H1–O_s^B	H1–O_s^B (0.096)	C1–O_s^A (0.140)	H_s transfer		−21.1	68.5
	C_2H_6	C1–O_s^A	H1–O_s^B	H1–O_s^B (0.096)	C1–O_s^A (0.142)	H_s transfer		−11.4	79.3
	C_5H_{12}	C1–O_s^A	H1–O_s^B	H1–O_s^B (0.096)	C1–O_s^A (0.141)	H_s transfer		−7.2	107.5
	CH_4	C1–O_s^{C1}	H1–O_s^{C2}	H1–O_s^{C2} (0.097)	C1–O_s^{C1} (0.139)			26.0	83.5
	C_2H_6	C1–O_s^{C1}	H1–O_s^{C2}	H1–O_s^{C2} (0.097)				54.9	83.2
	C_5H_{12}	C1–O_s^{C1}	H1–O_s^{C2}	H1–O_s^{C2} (0.097)				43.8	83.9
5		C1–Al_s & H1–O_s							
		C1–Al_s^A	H1–O_s^A	No reaction					
		C1–Al_s^C	H1–O_s^C	No reaction					
	CH_4	C1–Al_s^B	H1–O_s^B	H1–O_s^B (0.096)				42.7	78.5
	C_2H_6	C1–Al_s^B	H1–O_s^B	H1–O_s^B (0.096)				48.5	60.7
	C_5H_{12}	C1–Al_s^B	H1–O_s^B	No reaction					
6		H1–O_s^i & H2–O_s^j							
	C_2H_6	H1–O_s^B	H2–O_s^A	H1–O_s^B (0.096)	H2–O_s^A (0.096)	C=C (0.132)	H_s transfer	−23.4	56.0
	C_5H_{12}	H1–O_s^B	H2–O_s^A	H1–O_s^B (0.096)	H2–O_s^A (0.096)	C=C (0.133)	H_s transfer	−27.8	60.4
	C_2H_6	H1–O_s^{C1}	H2–O_s^{C2}	H1–O_s^{C1} (0.096)	H2–O_s^{C2} (0.097)	C=C (0.132)		18.1	77.8
	C_5H_{12}	H1–O_s^{C1}	H2–O_s^{C2}	H1–O_s^{C1} (0.097)	H2–O_s^{C2} (0.097)	C=C (0.133)		13.7	76.8
7	C_5H_{12}	H2–O_s		No reaction					
8	C_5H_{12}	H3–O_s		No reaction					
9		H2–O_s^i & H3–O_s^j							
	C_5H_{12}	H2–O_s^A	H3–O_s^B	H2–O_s^A (0.096)	H3–O_s^B (0.096)	C=C (0.133)	H_s transfer	−32.2	84.9
	C_5H_{12}	H2–O_s^{C1}	H3–O_s^{C2}	H2–O_s^{C1} (0.097)	H3–O_s^{C2} (0.097)	C=C (0.133)		9.2	73.5
Model II									
1		H1–O_s							
	CH_4	H1–O_s^A		H1–O_s^A (0.096)				−42.9	34.3
	C_2H_6	H1–O_s^A		H1–O_s^A (0.095)				−31.1	53.8
	C_5H_{12}	H1–O_s^A		H1–O_s^A (0.096)				−31.7	45.7
		H1–O_s^C		No reaction					
2		C1–O_s							
	CH_4	C1–O_s^{A1}		H1–O_s^{A2} (0.096)	C1–O_s^{A1} (0.139)			−96.3	25.5
	C_2H_6	C1–O_s^{A1}		H1–O_s^{A2} (0.096)	C1–O_s^{A1} (0.140)			−94.9	26.5
	C_5H_{12}	C1–O_s^{A1}		H1–O_s^{A2} (0.096)	C1–O_s^{A1} (0.140)			−84.7	33.6
		C1–O_s^C		No reaction					
3		H1–O_s & C1–O_s							
	CH_4	H1–O_s^{A1}	C1–O_s^{A1}	H1–O_s^{A2} (0.096)	C1–O_s^{A1} (0.137)			−96.0	50.0
	C_2H_6	H1–O_s^{A1}	C1–O_s^{A1}	H1–O_s^{A2} (0.096)	C1–O_s^{A1} (0.139)			−83.0	42.2
	C_5H_{12}	H1–O_s^{A1}	C1–O_s^{A1}	H1–O_s^{A2} (0.096)	C1–O_s^{A1} (0.139)			−86.4	42.4
	CH_4	H1–O_s^C	C1–O_s^C	H1–O_s^C (0.098)				26.7	68.3
	C_2H_6	H1–O_s^C	C1–O_s^C	H1–O_s^C (0.098)				45.5	68.8
	C_5H_{12}	H1–O_s^C	C1–O_s^C	H1–O_s^C (0.098)				32.7	101.0
4		C1–O_s^i & H1–O_s^j							
	CH_4	C1–O_s^{A1}	H1–O_s^{A2}	H1–O_s^{A2} (0.096)	C1–O_s^{A1} (0.139)			−96.8	40.0
	C_2H_6	C1–O_s^{A1}	H1–O_s^{A2}	H1–O_s^{A2} (0.096)	C1–O_s^{A1} (0.140)			−92.3	38.7
	C_5H_{12}	C1–O_s^{A1}	H1–O_s^{A2}	H1–O_s^{A2} (0.096)	C1–O_s^{A1} (0.140)			−89.4	45.6
	CH_4	C1–O_s^{C1}	H1–O_s^{C2}	H1–O_s^{C2} (0.098)				−12.9	126.5
	C_2H_6	C1–O_s^{C1}	H1–O_s^{C2}	H1–O_s^{C2} (0.098)				32.4	129.0

Table 1 (*Continued*)

No.	Alkane	Initial close contact		Bond formed			ΔE	ΔE_{act}
	C_5H_{12}	C1–O_s^{C1}	H1–O_s^{C2}	H1–O_s^{C2} (0.098)			47.0	141.6
5		C1–Al_s & H1–O_s						
a	CH_4	C1–Al_s	H1–O_s^{A1}	H1–O_s^{A2} (0.096)	C1–O_s^{A1} (0.139)		−96.5	27.6
a	C_2H_6	C1–Al_s	H1–O_s^{A1}	H1–O_s^{A2} (0.096)	C1–O_s^{A1} (0.140)		−84.2	54.8
a	C_5H_{12}	C1–Al_s	H1–O_s^{A1}	H1–O_s^{A2} (0.096)	C1–O_s^{A1} (0.140)		−89.2	45.4
b	CH_4	C1–Al_s	H1–O_s^{A}	H1–O_s^{A} (0.095)			−42.9	33.5
b	C_2H_6	C1–Al_s	H1–O_s^{A}	H1–O_s^{A} (0.095)			−20.2	33.0
b	C_5H_{12}	C1–Al_s	H1–O_s^{A}	H1–O_s^{A} (0.095)			−26.8	34.1
b	CH_4	C1–Al_s	H1–O_s^{C}	H1–O_s^{C} (0.098)			38.5	66.0
b	C_2H_6	C1–Al_s	H1–O_s^{C}	H1–O_s^{C} (0.098)			48.4	89.8
b	C_5H_{12}	C1–Al_s	H1–O_s^{C}	H1–O_s^{C} (0.098)			50.4	98.6
6		H1–O_s^{i} & H2–O_s^{j}						
	C_2H_6	H1–O_s^{A1}	H2–O_s^{A2}	H1–O_s^{A1} (0.096)	H2–O_s^{A2} (0.096)	C=C (0.132)	−115.6	37.2
	C_5H_{12}	H1–O_s^{A1}	H2–O_s^{A2}	H1–O_s^{A1} (0.096)	H2–O_s^{A2} (0.096)	C=C (0.133)	−115.4	36.8
	C_2H_6	H1–O_s^{C1}	H2–O_s^{C2}	H1–O_s^{C1} (0.099)	H2–O_s^{C2} (0.098)	C=C (0.134)	36.3	83.5
	C_5H_{12}	H1–O_s^{C1}	H2–O_s^{C2}	H1–O_s^{C1} (0.098)	H2–O_s^{C2} (0.099)	C=C (0.133)	28.9	68.3
7		H2–O_s						
	C_5H_{12}	H2–O_s^{A}		H2–O_s^{A} (0.096)			−6.4	47.7
	C_5H_{12}	H2–O_s^{C}		No reaction				
8		H3–O_s						
	C_5H_{12}	H3–O_s^{A}		H3–O_s^{A} (0.095)			−81.8	48.0
	C_5H_{12}	H3–O_s^{C}		No reaction				
9		H2–O_s^{i} & H3–O_s^{j}						
	C_5H_{12}	H2–O_s^{A1}	H3–O_s^{A2}	H2–O_s^{A1} (0.096)	H3–O_s^{A2} (0.096)	C=C (0.133)	−124.6	39.0
	C_5H_{12}	H2–O_s^{C1}	H3–O_s^{C2}	H2–O_s^{C1} (0.099)			79.0	93.0

$\Delta E = E$(alkane/substrate) − E(alkane) − E(substrate); ΔE_{act} is the activation energy of the reaction. The superscripts A1, A2, C1, C2 indicate different atoms on A and C sites.

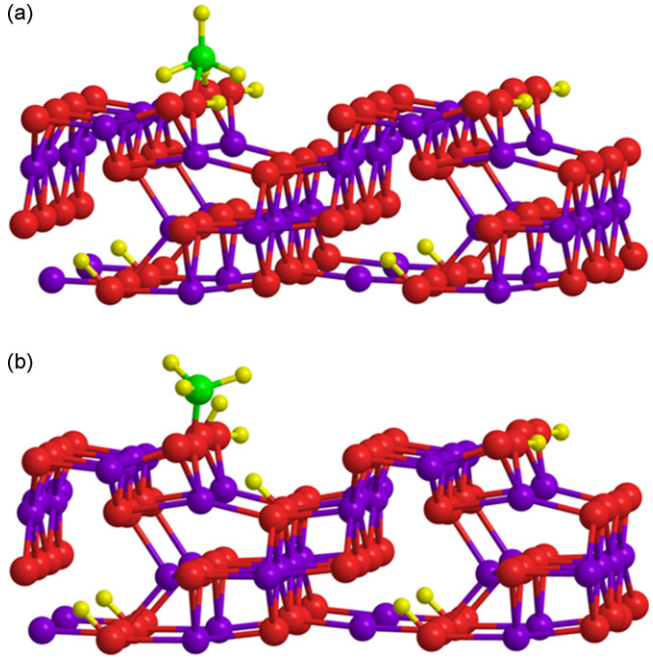

Fig. 3. Example interaction mode for methane. (a) Initial state configuration of C1–O_s^{A} & H1–O_s^{B} interaction; (b) final state configuration of C1–O_s^{A} & H1–O_s^{B} interaction. The purple, red, green, and yellow spheres represent Al, O, C, and H atoms, respectively. (For interpretation of the references to color in this figure legend, the reader is referred to the web version of the article.)

3.1.5. Interactions of C1 with a surface Al and H1 with a surface O atom

For initial configurations with C1 close to Al_s and H1 close to O_s, only the C1–Al_s^{B} & H1–O_s^{B} configuration for methane and ethane leads to reaction. This dehydrogenation is endothermic and proceeds with an activation energy of 78.5 and 60.7 kcal/mol for the two species, respectively. As we have shown in Section 3.1.1, reactions between only H and O_s do not happen. Therefore, the interaction of C with Al_s promotes the H1 abstraction. When we moved the CH_3 fragment to the surface so that d(C1 − Al_s^{B}) = 0.14 nm, upon full structural optimization the fragment leaves the surface again, indicating that the C1–Al_s interaction is repulsive.

3.1.6. Interactions of H1 and H2 with two different surface O atoms

Since methane contains no H2, this interaction mode only exists for ethane and pentane. Reactions happen for the H1–O_s^{B} & H2–O_s^{A} and H1–O_s^{C1} & H2–O_s^{C2} configurations. Both H1 and H2 are dehydrogenated, producing ethene or 1-pentene. The newly formed H–O_s bond lengths are about 0.097 nm. Similar to the methane reaction with configuration of C1–O_s & H1–O_s (Section 3.1.4), the reaction is endothermic with two O_s^{C}, and exothermic with O_s^{A} & O_s^{B}. The transfer of the H_s atom makes the latter reaction more favorable than the former one. The energy barrier to the latter reaction is also smaller than the former one.

3.1.7. Interactions of H2 with a surface O atom

When the initial configuration is such that one of the H2 atoms of pentane is in close proximity to a surface oxygen atom, upon full relaxation the molecule simply leaves the surface without any reaction.

3.1.8. Interactions of H3 with a surface O atom

When the initial configuration is such that one of the H3 atoms of pentane is in close proximity to a surface oxygen atom, upon full relaxation the molecule simply leaves the surface without any reaction.

3.1.9. Interactions of H2 and H3 with two different surface O atoms

This interaction mode only exists for pentane since only pentane has a C3 atom. Reactions happen for the H2–O_s^A & H3–O_s^B and H2–O_s^{C1} & H3–O_s^{C2} configurations. Both H2 and H3 are dehydrogenated, producing 2-pentene. The reaction is endothermic with two O_s^C, and exothermic with O_s^A & O_s^B due to the transfer of the H_s atom. The energy barrier to the exothermic reaction is slightly larger than that for the endothermic one.

3.2. Adsorption of methane and pentane on Model II

3.2.1. Interactions of H1 with a surface O atom

The interactions of H1 with a surface oxygen atom (O_s^A or O_s^C) were investigated. Reactions occur only for the H1–O_s^A interaction. In this case, the H1 atom transfers to the surface to form an H1–O_s bond with bond length ca. 0.096 nm, while the remnant fragment leaves the surface. The reactions are exothermic and the energy decrease is greatest for methane reaction. The energy barriers to be overcome before the reaction can happen are 34.3, 53.8 and 45.7 kcal/mol for methane, ethane and pentane, respectively. Fig. 2 gives corresponding energy variation curves with the H1–O_s distance for methane and pentane.

3.2.2. Interactions of C1 with a surface O atom

Similar to Section 3.2.1, reactions are only found on the O_s^A site. In addition to dehydrogenation, however, the remnant fragment also binds to the O_s^A atom forming a C1–O_s^A bond. Note that the abstracted H1 atom bonds to an O_s^A different from the one C1 bonds to. The reactions show gradually decreasing exothermicity from methane to pentane. By contrast, the energy barrier increases from methane to pentane. The energy barriers for these reactions are generally lower than those for the H1–O_s^A reactions.

3.2.3. Interactions of H1 and C1 with a surface O atom

The interactions of H1 and C1 with an O_s^A or O_s^C yield different results. For the interactions with O_s^A, the H1 is abstracted and bonds to an O_s^A atom, accompanied by the formation of a C1–O_s^A bond. This is similar to the case of pure C1–O_s^A interactions, including the final state energies but the energy barriers are higher for this reaction mode. For the interactions with O_s^C, however, only the H1 is transferred to the O_s^C, resulting in much higher energies in the final states than in the former case. These reactions are endothermic and the energy barriers are high, especially for pentane.

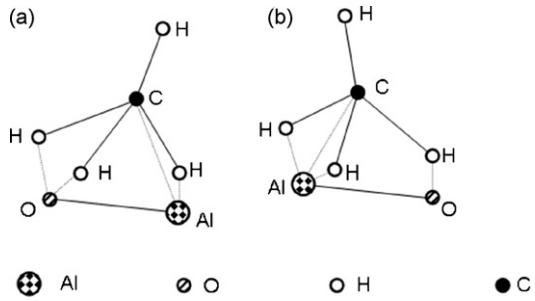

Fig. 4. Two multi-center interactions of a terminal –CH_3 with the alumina surface.

3.2.4. Interactions of H1 and C1 with two different surface O atoms

Similar to the interactions of H1 and C1 with a surface O atom (Section 3.2.3), the reactions on O_s^A sites result in dehydrogenation and formation of C1–O_s^A bond, while the reactions on O_s^C sites only result in dehydrogenation. The former reactions yield much more stable final state and require much lower activation energies.

3.2.5. Interactions of C1 with a surface Al and H1 with a surface O atom

There are two interaction modes of the type C1–Al_s & H1–O_s. In the first mode, one H1 and C1 are close to an Al_s and two H1 are close to an O_s (denoted as 'a' in column 1 of Table 1). In the second mode, two H1 and C1 are close to an Al_s and one H1 is close to an O_s (denoted as 'b' in column 1 of Table 1). Modes a and b are depicted in Fig. 4. For the interactions with Al_s & O_s^A, both modes a and b result in exothermic reactions, but the final products and final state energies are different. For mode b, the fragments resulting after dehydrogenation leave the surface, whereas they bond to O_s^A atoms in mode a. The final states of mode a reactions are more stable than those of the mode b reactions. Note that although for mode a, the H1–O_s^{A1} distance is smaller than the H1–O_s^{A2} distance in the initial configuration, the bond formed in the final product is H1–O_s^{A2}. For the interactions with Al_s & O_s^C in mode a, an H1 atom moves to a *boundary* O_s atom after structural relaxation. Since the boundary atoms are not described precisely in our model, this reaction is probably unphysical and is neglected in our discussion. In mode b, the reactions are endothermic and have larger barriers than the reactions on Al_s & O_s^A sites.

3.2.6. Interactions of H1 and H2 with different surface O atoms

The interactions of H1 and H2 with two O_s atoms were investigated. It was found that such interactions result in dehydrogenation of both the H1 and H2 atoms, with the product alkene leaving the surface. The new H–O_s bond lengths are about 0.1 nm. The energy of the final state for the reaction at sites O_s^A is lower than that of the corresponding free state $[E(\text{alkane}) + E(Al_{48}O_{72})]$, by about −115 kcal/mol for both

Table 2
Partial charges of surface oxygen (esu)

	O_s^A	O_s^B	O_s^C
Model I	−0.48	−0.66	−0.64 (av.)
Model II	−0.58 (av.)	–	−0.64 (av.)

ethane and pentane, whereas at sites O_s^C the final state energy is higher by 36.3 and 28.9 kcal/mol in the ethane and pentane cases, respectively. Fixing the H1 atom at various positions and relaxing all other atoms of the molecule, the energy barriers for such a reaction to happen were calculated to be much lower for the production of the alkene at the O_s^A site than at the O_s^C site.

3.2.7. Interactions of H2 with a surface O atom

The interactions of H2 with a surface oxygen atom (O_s^A or O_s^C) were investigated and found to produce a reaction only in the H2–O_s^A case. In this case, the reaction is slightly exothermic and a H2–O_s^A bond forms.

3.2.8. Interactions of H3 with a surface O atom

The interactions of H3 with a surface oxygen atom (O_s^A or O_s^C) are very similar to those of H2, except that the reactive case (H3–O_s^A) is much more exothermic than the H2–O_s^A case.

3.2.9. Interactions of H2 and H3 with different surface O atoms

The interaction of H2 and H3 with O_s^{A1} and O_s^{A2}, respectively, produces very similar results to those of H1 and H2 interacting with different O_s^A atoms. Such interaction results in dehydrogenation of both the H2 and H3 atoms, with the product 2-pentene leaving the surface. This is the most exothermic reaction for pentane overall, and has an energy barrier of only 39 kcal/mol. (This reaction mode is only possible for pentane, since only pentane has H3 atoms.) The interaction of H2 and H3 with O_s^{C1} and O_s^{C2}, respectively, produces only the formation of an H2–O_s^{C1} bond.

3.3. Surface O atoms

To further analyze the reactivity of surface Lewis base sites (O_s) we have computed Mopac charges, which are collected in Table 2. Note that O_s^A sites generally are less electron-rich than O_s^B and O_s^C sites.

4. Discussion

The low energy reaction modes are summarized in Table 3, where they are grouped by adsorbate and surface model, and ranked by decreasing exothermicity. It can be seen that on Model I, interactions of methane with the γ-alumina surface result in two types of reactions: abstraction of one H1 atom (type 1), and abstraction of one H1 atom accompanied by the formation of a C1–O bond (type 2). Only one reaction belonging to type 2 (C1–O_s^A & H1–O_s^B) is exothermic, and it also happens to have lowest energy barrier.

In the case of ethane interactions with the γ-alumina surface, three types of reactions are found. The lowest energy reaction is the dehydrogenation of H1 and H2 atoms, yielding ethene (type 3). The next most favorable reaction is the abstraction of one H1 atom accompanied by the formation of a C1–O bond (type 2), with type 1 reactions being the least favorable.

In the case of pentene interactions with the γ-alumina surface, four types of reactions are found. The lowest energy reaction is the dehydrogenation of H2 and H3 atoms, yielding 2-pentene (type 4). The next most favorable reaction is the dehydrogenation of H1 and H2 atoms, yielding 1-pentene (type 3). The least exothermic reaction is the abstraction of one H1 atom accompanied by the formation of a C1–O bond (type 2). Reaction type 1 is endothermic.

On Model II, type 2 reactions are more favorable than type 1 for methane, as is the case on Model I. Similarly, type 3 reaction is the most favorable and type 1 is the least favorable for ethane. For pentane, there are two new reaction types: abstraction of one H3 or one H2 atom. Among all six reaction types, reaction type 4 is the most favorable. As on model I, for interactions of pentane with Model II, reactions of type 2 are more favorable than those of type 1. Almost all reactions happen on site O_s^A, indicating the relative inertness of site O_s^C.

Since the hydrogenated model (Model I) is probably more representative of low-temperature catalyst operation and the hydrogen-free model (Model II) is probably more representative of high-temperature catalyst operation, it can be concluded that independent of temperature, the interaction of methane with the γ-alumina surface results in the abstraction of one H atom accompanied by the formation of a C–O bond. For the other alkanes, however, the main reactions are the formation of an alkene by the dehydrogenation of two H atoms. On both models, sites O_s^A and O_s^B are generally more reactive than site O_s^C.

In the case of pentane, the calculations find production of 2-pentene to slightly more exothermic that production of 1-pentene. This is consistent with the fact that the terminal alkene is the thermodynamically less stable of the two isomers as is shown by the experimental observation that hydrogenation of 1-pentene is exothermic by 30.1 kcal/mol, hydrogenation of *trans*-2-pentene is exothermic by 27.6 kcal/mol, and hydrogenation of *cis*-2-pentene is exothermic by 28.6 kcal/mol [29]. The computed energy barriers, however, suggest that production of the terminal alkene is kinetically favored. While the small difference between the barriers to production of 1-pentene and 2-pentene is less than the degree of uncertainty from the PM3 methodology, there is some experimental evidence that supports this prediction. According to Ref. [30] reaction of pentane on a Cr–K-doped alumina catalyst at 527 K produced 9.7% 1-pentene and 90.3% is 2-pentene. Based on the relative energies of the pentene isomers determined from the hydrogenation reactions cited above, an equilibrium Boltzmann distribution at 527 K will contain only 6.2% 1-pentene and 93.8% 2-pentene. The reaction is actually producing more 1-pentene than is predicted based strictly on equilibrium thermodynamic considerations. This suggests that there is in fact a slight kinetic preference for production of 1-pentene over 2-pentene. (One caveat to this analysis is that the experimental

Table 3
List of low energy reaction modes (energies in kcal/mol)

Reaction mode	Products	ΔE	ΔE_{act}
Model I			
CH_4			
C1–O_s^{A} & H1–O_s^{B}	H1–O_s^{B}, C1–O_s^{A}, H_s transfer	−21.1	68.5
C1–O_s^{C1} & H1–O_s^{C2}	H1–O_s^{C2}, C1–O_s^{C1}	26.0	83.5
H1–O_s^{A} & C1–O_s^{A}	H1–O_s^{A}, C1–O_s^{A}, H_s transfer	31.5	94.2
C1–Al_s^{B} & H1–O_s^{B}	H1–O_s^{B}	42.7	78.5
C_2H_6			
H1–O_s^{B} & H2–O_s^{A}	H1–O_s^{B}, H2–O_s^{A}, C=C, H_s transfer	−23.4	56.0
C1–O_s^{A} & H1–O_s^{B}	H1–O_s^{B}, C1–O_s^{A}, H_s transfer	−11.4	79.3
H1–O_s^{C1} & H2–O_s^{C2}	H1–O_s^{C1}, H2–O_s^{C2}, C=C	18.1	77.8
H1–O_s^{A} & C1–O_s^{A}	H1–O_s^{A}, C1–O_s^{A}, H_s transfer	40.7	101.4
C1–Al_s^{B} & H1–O_s^{B}	H1–O_s^{B}	48.5	60.7
C1–O_s^{C1} & H1–O_s^{C2}	H1–O_s^{C2}	54.9	83.2
C_5H_{12}			
H2–O_s^{A} & H3–O_s^{B}	H2–O_s^{A}, H3–O_s^{B}, C=C, H_s transfer	−32.2	84.9
H1–O_s^{B} & H2–O_s^{A}	H1–O_s^{B}, H2–O_s^{A}, C=C, H_s transfer	−27.8	60.4
C1–O_s^{A} & H1–O_s^{B}	H1–O_s^{B}, C1–O_s^{A}, H_s transfer	−7.2	107.5
H2–O_s^{C1} & H3–O_s^{C2}	H2–O_s^{C1}, H3–O_s^{C2}, C=C	9.2	73.5
H1–O_s^{C1} & H2–O_s^{C2}	H1–O_s^{C1}, H2–O_s^{C2}, C=C	13.7	76.8
C1–O_s^{C1} & H1–O_s^{C2}	H1–O_s^{C2}	43.8	83.9
H1–O_s^{A} & C1–O_s^{A}	H1–O_s^{A}, C1–O_s^{A}, H_s transfer	44.1	107.7
Model II			
CH_4			
C1–O_s^{A1} & H1–O_s^{A2}	H1–O_s^{A2}, C1–O_s^{A1}	−96.8	40.0
C1–Al_s & H1–O_s^{A1} (a)	H1–O_s^{A2}, C1–O_s^{A1}	−96.5	27.6
C1–O_s^{A1}	H1–O_s^{A2}, C1–O_s^{A1}	−96.3	25.5
H1–O_s^{A1} & C1–O_s^{A1}	H1–O_s^{A2}, C1–O_s^{A1}	−96.0	50.0
H1–O_s^{A}	H1–O_s^{A}	−42.9	34.3
C1–Al_s & H1–O_s^{A} (b)	H1–O_s^{A}	−42.9	33.5
C1–O_s^{C1} & H1–O_s^{C2}	H1–O_s^{C2}	−12.9	126.5
C_2H_6			
H1–O_s^{A1} & H2–O_s^{A2}	H1–O_s^{A1}, H2–O_s^{A2}, C=C	−115.6	37.2
C1–O_s^{A1}	H1–O_s^{A2}, C1–O_s^{A1}	−94.9	26.5
C1–O_s^{A1} & H1–O_s^{A2}	H1–O_s^{A2}, C1–O_s^{A1}	−92.3	38.7
C1–Al_s & H1–O_s^{A1} (a)	H1–O_s^{A2}, C1–O_s^{A1}	−84.2	54.8
H1–O_s^{A1} & C1–O_s^{A1}	H1–O_s^{A2}, C1–O_s^{A1}	−83.0	42.2
H1–O_s^{A}	H1–O_s^{A}	−31.1	53.8
C1–Al_s & H1–O_s^{A} (b)	H1–O_s^{A}	−20.2	33.0
C_5H_{12}			
H2–O_s^{A1} & H3–O_s^{A2}	H2–O_s^{A1}, H3–O_s^{A2}, C=C	−124.6	39.0
H1–O_s^{A1} & H2–O_s^{A2}	H1–O_s^{A1}, H2–O_s^{A2}, C=C	−115.4	36.8
C1–O_s^{A1} & H1–O_s^{A2}	H1–O_s^{A2}, C1–O_s^{A1}	−89.4	45.6
C1–Al_s & H1–O_s^{A1} (a)	H1–O_s^{A2}, C1–O_s^{A1}	−89.2	45.4
H1–O_s^{A1} & C1–O_s^{A1}	H1–O_s^{A2}, C1–O_s^{A1}	−86.4	42.4
C1–O_s^{A1}	H1–O_s^{A2}, C1–O_s^{A1}	−84.7	33.6
H3–O_s^{A}	H3–O_s^{A}	−81.8	48.0
H1–O_s^{A}	H1–O_s^{A}	−31.7	45.7
C1–Al_s & H1–O_s^{A} (b)	H1–O_s^{A}	−26.8	34.1
H2–O_s^{A}	H2–O_s^{A}	−6.4	47.7

results are not for a pure alumina catalyst, as are our calculations.)

Our results suggest that H/D exchange is most probably initiated by dissociative methane chemisorption over Lewis base sites. Although Lewis acid sites may be involved in promoting the dissociation, the CD_3 moiety is bound to an O atom of Lewis base character, not to surface aluminum as has been proposed previously [5,6].

5. Conclusions

In conclusion, we have employed semi-empirical (PM3) cluster calculations to investigate the adsorptions of methane, ethane and pentane on the γ-alumina (110C) surface. The results show that regardless of the hydrogenation of the alumina, all three alkanes can be dehydrogenated when they come sufficiently close to the surface. The main product of methane–alumina reac-

tions leaves the CH_3 moiety bound to a surface O atom that is coordinated by two Al atoms ($O_s{}^A$ or $O_s{}^B$). By contrast, the main products for ethane– and pentane–alumina interactions are the corresponding alkenes.

Acknowledgments

This work was supported by DuPont and by NATO-PST-CLG-980354. The authors thank M. Caldararu and C. Horniou for valuable discussions regarding reaction mechanisms.

References

[1] T.N. Truong, J. Phys. Chem. B 101 (1997) 2750.
[2] J.M. Vollmer, T.N. Truong, J. Phys. Chem. B 104 (2000) 6308.
[3] C.J.A. Mota, J. Sommer, M. Hachoumy, R. Jost, J. Catal. 172 (1997) 194.
[4] J. Sommer, D. Habermacher, R. Jost, A. Sassi, A.G. Stepanov, M.V. Luzgin, D. Freude, H. Ernst, J. Martens, J. Catal. 181 (1999) 265.
[5] J. Engelhardt, J. Valyon, React. Kinet. Catal. Lett. 74 (2001) 217.
[6] J. Valyon, J. Engelhardt, D. Kallo, M. Hegedus, Catal. Lett. 82 (2002) 29.
[7] H. Tachikawa, T. Tsuchida, J. Mol. Catal. A 96 (1995) 277.
[8] M.B. Fleisher, L.O. Golender, M.V. Shimanskaya, J. Chem. Soc., Faraday Trans. 87 (1991) 745.
[9] H. Kawakami, S. Yoshida, J. Chem. Soc., Faraday Trans. 81 (1985) 1117.
[10] O. Maresca, A. Allouche, J.P. Aycard, M. Rajzmann, S. Clemendot, F. Hutschka, J. Mol. Struct. (Theochem) 505 (2000) 81.
[11] P. Hirva, T.A. Pakkanen, Surf. Sci. 277 (1992) 389.
[12] M. Lindblad, T.A. Pakkanen, Surf. Sci. 286 (1993) 333.
[13] D.A. De Vito, F. Gilardoni, L. Kiwi-Minsker, P.Y. Morgantini, S. Porchet, A. Renken, J. Weber, J. Mol. Struct. (Theochem) 469 (1999) 7.
[14] S.H. Cai, K. Sohlberg, J. Mol. Catal. A 248 (2006) 76.
[15] S.H. Cai, K. Sohlberg, J. Mol. Catal. A 193 (2003) 157.
[16] J.J.P. Stewart, J. Comput. Chem. 10 (1989) 209.
[17] J.J.P. Stewart, J. Comput. Chem. 10 (1989) 221.
[18] K. Sohlberg, S.T. Pantelides, S.J. Pennycook, J. Am. Chem. Soc. 123 (2001) 26.
[19] E.P. Smirnov, A.A. Tsyganenko, React. Kinet. Catal. Lett. 7 (1977) 425.
[20] E.P. Smirnov, A.A. Tsyganenko, React. Kinet. Catal. Lett. 26 (1984) 405.
[21] R.S. Zhou, R.L. Snyder, Acta Crystallogr. B 47 (1991) 617.
[22] K. Sohlberg, S.J. Pennycook, S.T. Pantelides, J. Am. Chem. Soc. 121 (1999) 7493.
[23] H. Knozinger, P. Ratnasamy, Catal. Rev. Sci. Eng. 17 (1978) 31.
[24] Y. Chen, L.F. Zhang, Catal. Lett. 12 (1992) 51.
[25] P.D. Nellist, S.J. Pennycook, Science 274 (1996) 413.
[26] K. Sohlberg, S.J. Pennycook, S.T. Pantelides, J. Am. Chem. Soc. 121 (1999) 10999.
[27] L.J. Alvarez, J.F. Sanz, M.J. Capitan, M.A. Centeno, J.A. Odriozola, J. Chem. Soc., Faraday Trans. 89 (1993) 3623.
[28] D. Coster, A.L. Blumenfeld, J.J. Fripiat, J. Phys. Chem. 98 (1994) 6201.
[29] T.W.G. Solomons, Organic Chemistry, Wiley, New York, 1980.
[30] N.I. Shuikin, E.A. Timofeeva, V.M. Kleimenova, Russ. Chem. Bull. 6 (1957) 903.